Bright single photon source based on self-aligned quantum dot–cavity systems

Sebastian Maier,[1,*] Peter Gold,[1] Alfred Forchel,[1] Niels Gregersen,[2] Jesper Mørk,[2] Sven Höfling,[1,3] Christian Schneider,[1,4] and Martin Kamp[1]

[1]*Technische Physik, Physikalisches Institut and Wilhelm Conrad Röntgen-Research Center for Complex Material Systems, Universität Würzburg, Am Hubland, D-97074, Würzburg, Germany*

[2]*DTU Fotonik, Department of Photonics Engineering, Technical University of Denmark, Building 343, DK-2800 Kongens Lyngby, Denmark*

[3]*Present address: SUPA, School of Physics and Astronomy, University of St Andrews, St Andrews, KY16 9SS, UK*

[4]*christian.schneider@physik.uni-wuerzburg.de*

[*]*sebastian.maier@physik.uni-wuerzburg.de*

Abstract: We report on a quasi-planar quantum-dot-based single-photon source that shows an unprecedented high extraction efficiency of 42% without complex photonic resonator geometries or post-growth nanofabrication. This very high efficiency originates from the coupling of the photons emitted by a quantum dot to a Gaussian shaped nanohill defect that naturally arises during epitaxial growth in a self-aligned manner. We investigate the morphology of these defects and characterize the photonic operation mechanism. Our results show that these naturally arising coupled quantum dot-defects provide a new avenue for efficient (up to 42% demonstrated) and pure ($g^2(0)$ value of 0.023) single-photon emission.

OCIS codes: (230.5590) Quantum-well, -wire and -dot devices; (230.5750) Resonators; (270.5290) Photon statistics; (270.5565) Quantum communications.

References and links

1. N. Gisin, G. Ribordy, W. Tittel, and H. Zbinden, "Quantum cryptography," Rev. Mod. Phys. **74**(1), 145–195 (2002).
2. S. Strauf, "Quantum optics: Towards efficient quantum sources," Nat. Photonics **4**(3), 132–134 (2010).
3. E. Knill, R. Laflamme, and G. J. Milburn, "A scheme for efficient quantum computation with linear optics," Nature **409**(6816), 46–52 (2001).
4. M. Bayer, O. Stern, P. Hawrylak, S. Fafard, and A. Forchel, "Hidden symmetries in the energy levels of excitonic 'artificial atoms'," Nature **405**(6789), 923–926 (2000).
5. N. Gregersen, P. Kaer, and J. Mørk, "Modeling and design of high-efficiency single-photon sources," IEEE J. Sel. Top. Quantum Electron. **19**(5), 9000516 (2013).
6. T. Heindel, C. Schneider, M. Lermer, S. H. Kwon, T. Braun, S. Reitzenstein, S. Höfling, M. Kamp, and A. Forchel, "Electrically driven quantum dot-micropillar single photon source with 34% overall efficiency," Appl. Phys. Lett. **96**(1), 011107 (2010).
7. M. Pelton, C. Santori, J. Vucković, B. Zhang, G. S. Solomon, J. Plant, and Y. Yamamoto, "Efficient source of single photons: a single quantum dot in a micropost microcavity," Phys. Rev. Lett. **89**(23), 233602 (2002).
8. O. Gazzano, S. Michaelis de Vasconcellos, C. Arnold, A. Nowak, E. Galopin, I. Sagnes, L. Lanco, A. Lemaître, and P. Senellart, "Bright solid-state sources of indistinguishable single photons," Nat. Commun. **4**, 1425 (2013).
9. J. Claudon, J. Bleuse, N. S. Malik, M. Bazin, P. Jaffrennou, N. Gregersen, C. Sauvan, P. Lalanne, and J.-M. Gérard, "A highly efficient single-photon source based on a quantum dot in a photonic nanowire," Nat. Photonics **4**(3), 174–177 (2010).
10. M. E. Reimer, G. Bulgarini, N. Akopian, M. Hocevar, M. B. Bavinck, M. A. Verheijen, E. P. A. M. Bakkers, L. P. Kouwenhoven, and V. Zwiller, "Bright single-photon sources in bottom-up tailored nanowires," Nat. Commun. **3**, 737 (2012).
11. X.-W. Chen, S. Götzinger, and V. Sandoghdar, "99% efficiency in collecting photons from a single emitter," Opt. Lett. **36**(18), 3545–3547 (2011).
12. D. Press, K. De Greve, P. L. McMahon, T. D. Ladd, B. Friess, C. Schneider, M. Kamp, S. Höfling, A. Forchel, and Y. Yamamoto, "Ultrafast optical spin echo in a single quantum dot," Nat. Photonics **4**(6), 367–370 (2010).
13. K. De Greve, D. Press, P. L. McMahon, and Y. Yamamoto, "Ultrafast optical control of individual quantum dot spin qubits," Rep. Prog. Phys. **76**(9), 092501 (2013).

#205981 - $15.00 USD Received 4 Feb 2014; revised 13 Mar 2014; accepted 14 Mar 2014; published 31 Mar 2014

14. P. Royo, R. P. Stanley, and M. Ilegems, "Planar dielectric microcavity light-emitting diodes: Analytical analysis of the extraction efficiency," J. Appl. Phys. **90**(1), 283–293 (2001).
15. J. M. García, T. Mankad, P. O. Holtz, P. J. Wellman, and P. M. Petroff, "Electronic states tuning of InAs self-assembled quantum dots," Appl. Phys. Lett. **72**(24), 3172–3174 (1998).
16. J. M. Zajac and W. Langbein, "Structure and zero-dimensional polariton spectrum of natural defects in GaAs/AlAs microcavities," Phys. Rev. B **86**(19), 195401 (2012).
17. F. Ding, T. Stöferle, L. Mai, A. Knoll, and R. F. Mahrt, "Vertical microcavities with high Q and strong lateral mode confinement," Phys. Rev. B **87**(16), 161116 (2013).
18. L. Mai, F. Ding, T. Stöferle, A. Knoll, B. J. Offrein, and R. F. Mahrt, "Integrated vertical microcavity using a nano-scale deformation for strong lateral confinement," Appl. Phys. Lett. **103**(24), 243305 (2013).
19. O. El Daïf, A. Baas, T. Guillet, J.-P. Brantut, R. Idrissi Kaitouni, J. L. Staehli, F. Morier-Genoud, and B. Deveaud, "Polariton quantum boxes in semiconductor microcavities," Appl. Phys. Lett. **88**(6), 061105 (2006).
20. C. Santori, D. Fattal, J. Vucković, G. S. Solomon, and Y. Yamamoto, "Indistinguishable photons from a single-photon device," Nature **419**(6907), 594–597 (2002).
21. P. Gold, A. Thoma, S. Maier, S. Reitzenstein, C. Schneider, S. Höfling, and M. Kamp, "Two-photon interference from remote quantum dots with inhomogeneously broadened linewidths," Phys. Rev. B **89**(3), 035313 (2014).
22. P. Bienstman and R. Baets, "Optical modelling of photonic crystals and VCSELs using eigenmode expansion and perfectly matched layers," Opt. Quantum Electron. **33**(4–5), 327–341 (2001).

Bright sources of single and indistinguishable photons are of great interest in the field of quantum key distribution [1], quantum optics [2], and linear optical quantum computing [3]. Single semiconductor quantum dots (QDs) are promising candidates for this purpose, as they behave like artificial atoms [4]. However, efficient light outcoupling is critical and many sample designs [5] have been explored to maximize extraction efficiencies, such as micropillar cavities [6–8], photonic nanowires [9,10] and planar dielectric antennas [11]. Planar single-photon sources are of particular interest for spin manipulation experiments in order to avoid etched surfaces [12], which lead to spin dephasing. Furthermore a two-dimensional planar QD array can serve as basis for the realization of an optically controlled 2-qubit scheme [13].

Here we demonstrate a quantum-dot-based single-photon source based on a simple planar low quality factor cavity with an experimentally determined extraction efficiency of 42% ± 5%. The high efficiency is caused by the self-aligned formation of oval nanohill defects on top of the QDs. It significantly exceeds the maximum for the extraction efficiency from planar bulk GaAs semiconductor structures (~2%) and planar DBR microcavities without lateral optical confinement (~30%) [14]. Our sample was fabricated via molecular beam epitaxy (MBE) and contains a λ-thick cavity, which is sandwiched between two distributed Bragg reflector (DBRs), consisting of 18 (5) bottom (top) layers of AlAs/GaAs mirror pairs (MPs). The asymmetric design with a planar Q factor of about 200 is optimized for enhanced light outcoupling. The modulation doped low density In(Ga)As QDs are centered in the GaAs cavity and are spectrally shifted to the 900 nm range by using the Indium flush technique [15]. The microcavity layers were designed to accomplish spectral matching between the QD emission band and the optical resonance.

#205981 - $15.00 USD Received 4 Feb 2014; revised 13 Mar 2014; accepted 14 Mar 2014; published 31 Mar 2014

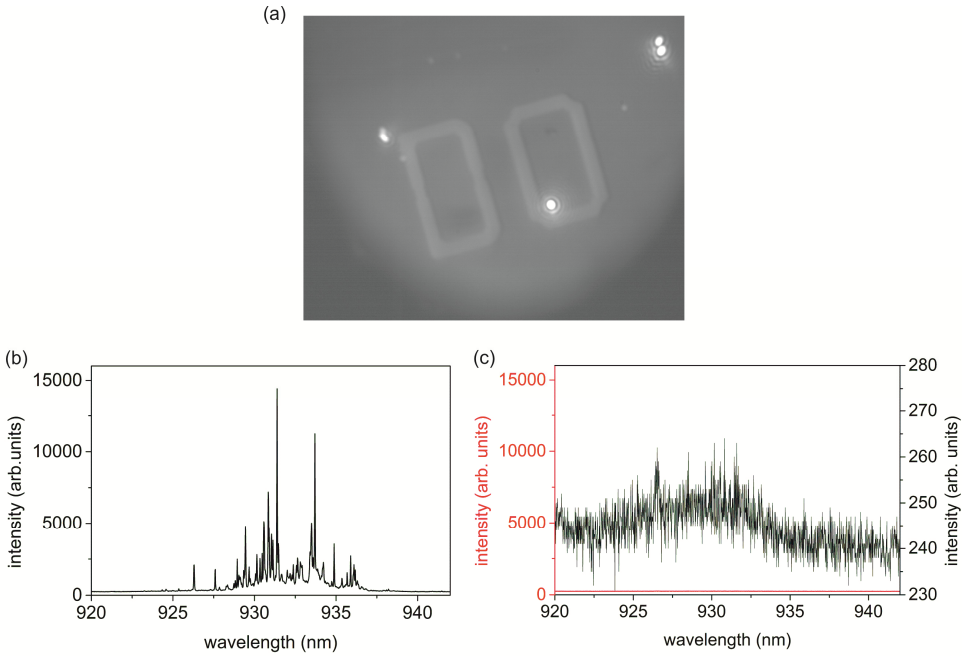

Fig. 1. (a) Surface image of CCD camera under white light excitation of the sample and use of a cold light mirror, revealing spots of very intense QD emission. The grey letter in the background serves for orientation on the sample. (b) µPL spectrum of a QD cluster. (c) µPL spectrum next to a QD cluster under the same conditions (red). The black curve shows the same spectrum with a rescaled axis.

Figure 1(a) shows a magnified section of the surface of the sample (at a temperature of 10 K) under illumination with a white light lamp and use of a cold mirror as longpass filter (cut-on wavelength at 750 nm). Very intense spots of near infrared light emission can be recognized on a CCD camera and are attributed to emission features from particularly bright QDs. Figure 1(b) shows the micro photoluminescence (µPL) spectrum of one of these QD clusters under excitation of a cw laser at 532 nm and 1 s integration time. The collection spot has a diameter on the order of 3 µm and we estimate that about 10 QDs contribute to the emission. The PL analysis of the spectral distribution of the QD ensemble (FWHM of about 17 meV) and spectral position of the cavity resonance (FWHM of about 8 meV) under several nanohill defects enables the estimation of the yield of spectrally resonant QD-cavity systems. From the number of QDs which are on resonance with the cavity (spectral position inside the range of the FWHM) and the number of QDs of the whole ensemble, we calculate a yield of about 33%. A spectrum recorded under the same excitation conditions, but next to these spots shows no characteristic QD lines as shown in Fig. 1(c).

To investigate the surface of the areas on the sample where the bright QD emission is measured, atomic force microscopy (AFM) was performed. The AFM image in Fig. 2(a) shows the sample surface above such a QD cluster which indicates the presence of an incidentally formed crystal defect which evolved during MBE growth. Detailed analysis of the measurement in Figs. 2(b) and 2(c) reveals an oval structure which is oriented along the (0-11) direction. Its dimensions amount to approximately 3.5 µm length, 800 nm width and 14 nm in height. The formation of lateral optical confinement via oval defect structures in quasi-planar microcavities has already been observed [16] and it is known that oval defects occur when Ga droplets are formed during MBE growth.

#205981 - $15.00 USD Received 4 Feb 2014; revised 13 Mar 2014; accepted 14 Mar 2014; published 31 Mar 2014

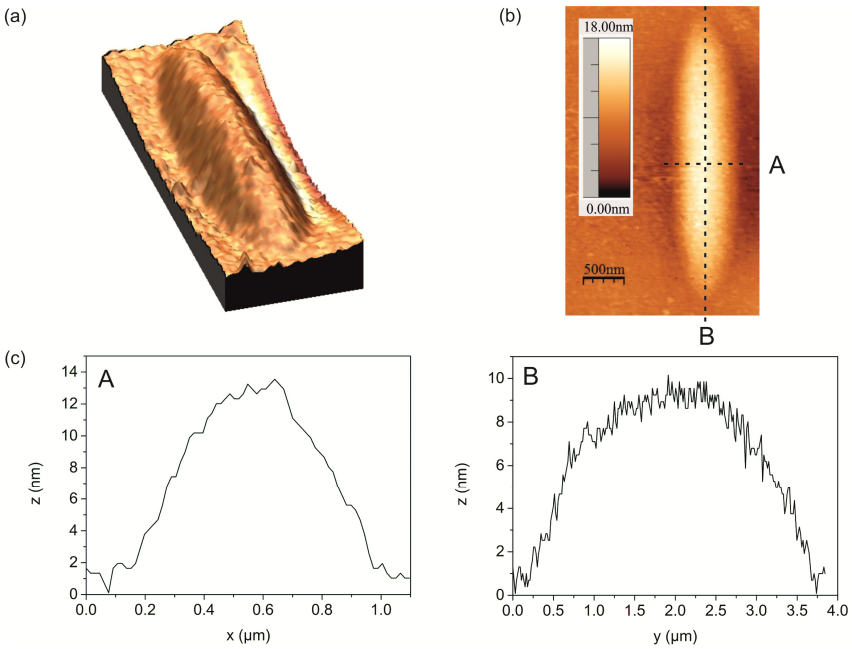

Fig. 2. (a), (b) Atomic force microscopy measurements reveal oval defects. (c) Cross sectional height distribution of the oval defects.

The propagation of the dislocation of the mirror pairs through the DBR results in a natural nearly Gaussian-shaped trap structure, which was recently proposed as a new concept for lateral photon confinement [17,18]. As QDs are likely to be formed on surface dislocations, the QDs are self-aligned in the natural defect structure, which is very important as it enables scalability of the sample design. This statement is underlined by the absence of any characteristic QD features next to the defect structures as shown in Fig. 1(c). While a deterministic fabrication of aligned QDs to random oval crystal defects is challenging as it requires a high degree of control over both, the QD nucleation and the defect formation, we would like to note that a lithographic definition of defects in the cavity layer has been demonstrated [18,19]. A combination of such a scheme with site-controlled QD growth routines would lead to a fully scalable and reproducible approach to fabricate highly efficient, quasi-planar single QD single photon sources.

Figure 3(a) shows a photoluminescence spectrum of a spectrally well isolated QD exciton in a natural trap structure under pulsed p-shell excitation. The single-photon emission characteristics were investigated by measuring the second order auto-correlation function in a standard Hanbury Brown and Twiss (HBT) setup. The QD was excited into the p-shell by a ps-pulsed Ti:sapphire Laser with a pulse separation of 12.2 ns at a wavelength of 911 nm. We calculate a $g^2(0)$ value of 0.023 from the raw data, which is depicted in Fig. 3(b) without any background corrections by dividing the number of counts in the range of ± 6.1 ns around zero delay time by the average number of counts of the peaks. These measurements demonstrate the high purity of the single-photon source and the excellent quality of the quantum emitter.

#205981 - $15.00 USD Received 4 Feb 2014; revised 13 Mar 2014; accepted 14 Mar 2014; published 31 Mar 2014

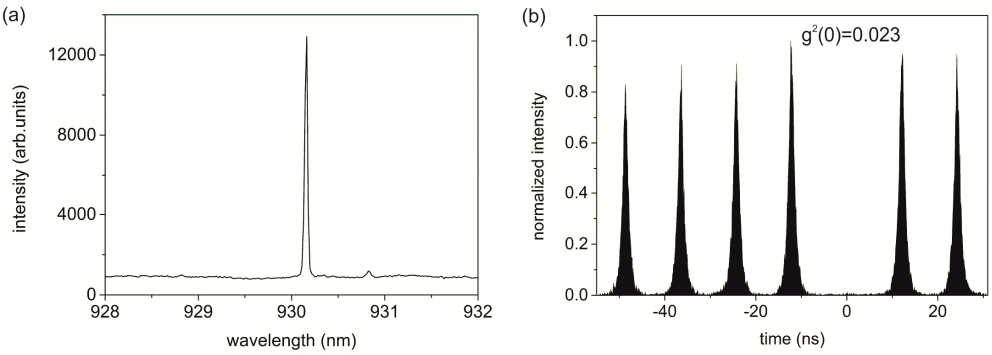

Fig. 3. (a) μPL spectrum (measured at 6 K) of a single QD in a natural trap. (b) Second order auto-correlation function measured in a Hanbury Brown and Twiss setup under pulsed excitation.

The extraction efficiency of the single photon source is measured at saturation of the QD-exciton: The QD emission is coupled to an avalanche photo diode (APD) using a microscope objective with a numerical aperture of NA = 0.7. We compare the photon counts per second on the single photon detectors (relative error 4%) with the laser repetition frequency of 82 MHz under consideration of the optical losses in the beam path due to an imperfect setup efficiency. The overall setup efficiency is assessed by using pulsed laser light of known power, which is tuned to the wavelength of the exciton (930 nm) and reflected from a gold mirror inside the cryostat. The photon counts per second on the single photon detectors are measured under the same setup conditions that we use for the single photon source, except for an additional density filter. We calculate the overall setup efficiency by comparing the laser photon flux, reflected on the gold mirror, with the maximum count rates on the APD, considering the transmission of the additional density filters. We find an overall detection efficiency of $(0.35 \pm 0.04)\cdot 10^{-3}$. Furthermore, all optical elements on the detection path have been calibrated with a continuous wave laser at the same wavelength. Table 1 shows a compilation of the transmission of these optical elements with relative errors. Considering the finite $g^2(0)$ value the efficiency of the single photon source amounts to 42% ± 5%.

Table 1. Transmission of the optical elements in the detection path with relative errors.

	transmission	error
Cryostat window + microscope objective	0.14	± 4%
silver mirrors	0.67	± 4%
50/50 NPBS	0.46	± 4%
Achromatic lens	0.91	± 4%
Bandpas filter	0.71	± 4%
Detection efficiency	0.013	± 5%
Setup efficiency	0.00035	± 10%

NPBS: non polarizing beam splitter. The measurement was performed with a continuous wave laser of known power at a wavelength of 930 nm. The detection efficiency includes the spectrometer transmission, the coupling lenses, incoupling into the single mode fiber based HBT and the APD efficiency.

#205981 - $15.00 USD Received 4 Feb 2014; revised 13 Mar 2014; accepted 14 Mar 2014; published 31 Mar 2014

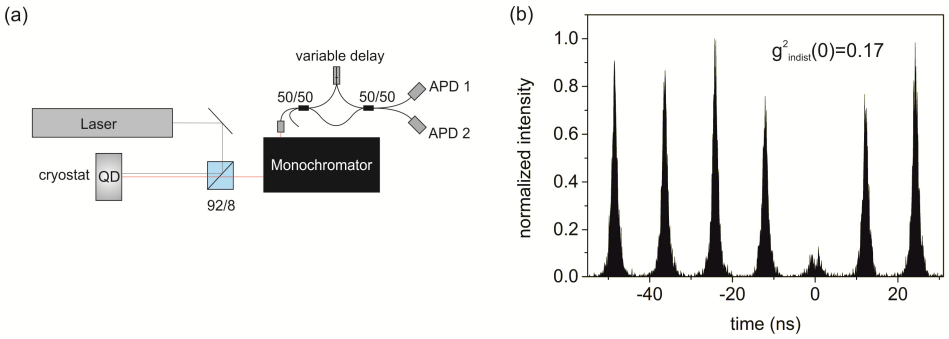

Fig. 4. Hong-Ou-Mandel experiment: (a) Schematic drawing of the interference setup. (b) Correlation histogram for two photon interference of consecutively emitted photons from the same QD.

This bright single-photon source was used to measure two photon interference in a Hong-Ou-Mandel (HOM) setup as shown schematically in Fig. 4(a). The laser is tuned to a wavelength of 911 nm and the QD is driven via pulsed p-shell excitation. After spectral filtering with a monochromator, the QD emission is coupled into the first 50/50 fiber beamsplitter of the HOM interferometer. In order to facilitate the interference of consecutively emitted photons on the second 50/50 fiber beamsplitter, we include a variable optical fiber delay in one of the two arms of the interferometer, which is adapted to the pulse separation and additionally allows us to fine adjust the time difference Δt between two photons. Figure 4(b) shows the two photon interference correlation histogram at an interferometer path length difference of $\Delta t \approx 0$. From the raw data we calculate a $g^2_{indist}(0)$ value of 0.17<0.50, which clearly shows indistinguishability of two consecutively emitted photons from the same QD [20] with a visibility of 66%. The exciton lifetime (T1) and coherence time (T2) of this QD amount to 670 ps and 330 ps, as extracted from time resolved measurements and Michelson interferometry. Despite being far away from the fourier limit, the rather high interference visibilities extracted from the two photon interference measurements lead us to the conclusion, that the spectral broadening mechanisms leading to a reduction of the coherence time assessed in the interferometric experiment occurs on a timescale larger than 12.2 ns, i.e the repetition rate of our pump laser. A detailed discussion of the effects of spectral broadening on the interference properties of single photons emitted from such QDs can be found in [21].

To calculate the theoretical extraction efficiency of a planar DBR structure and a radial symmetric defect structure, we performed full 3D vectorial simulations based on the eigenmode expansion technique [22]. Figure 5(a) shows the electric field amplitude profile in the case of a planar DBR structure with 18 (5) bottom (top) MPs. The maximum extraction efficiency at an emission wavelength of 940 nm is 33% for NA = 0.7, as depicted in Fig. 5(d), in agreement with previous reports [14]. The defect was modeled as a radial symmetric trap structure with a radius of 1000 nm and a slight variation in height as shown in Fig. 5(b). In Fig. 5(c) the electric field amplitude profile for the defect structure is depicted. Substantially more light is guided to the surface due to lensing effects provided by the defect. The simulation of the collection efficiency in Fig. 5(d) clearly shows an improvement of light outcoupling in the spectral range of the cavity resonance. For a defect height of 20 nm and a wavelength of 932 nm the theoretical extraction efficiency amounts to 48% which is in good accordance with the experimentally measured value.

#205981 - $15.00 USD Received 4 Feb 2014; revised 13 Mar 2014; accepted 14 Mar 2014; published 31 Mar 2014

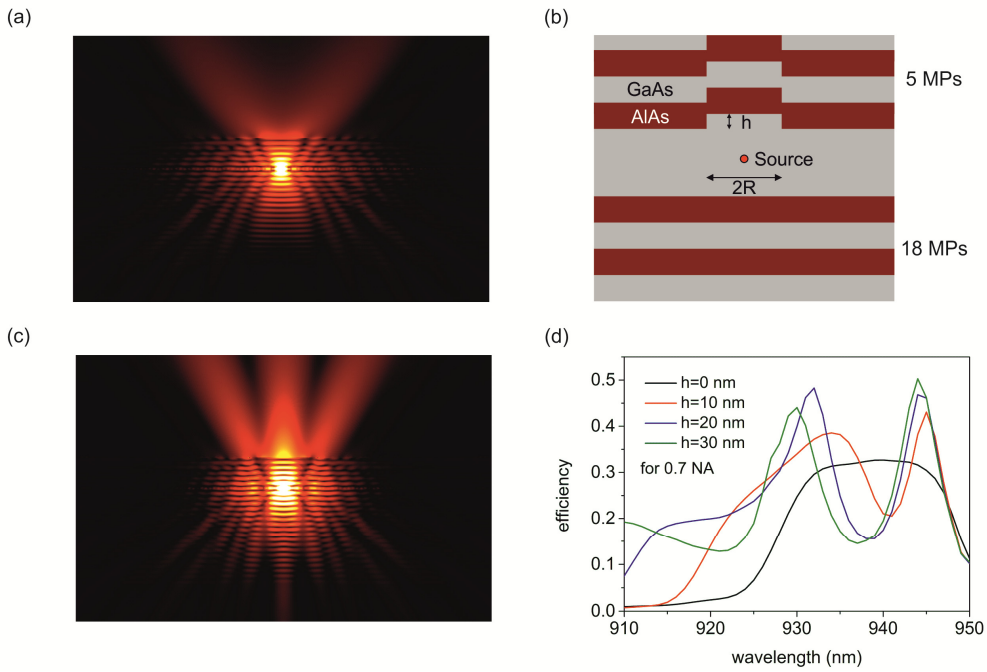

Fig. 5. Simulation results: (a) Electric field amplitude profile of the planar DBR structure. (b) Schematic drawing of the simulation layout. (c) Electric field amplitude profile of the defect structure. (d) Simulated extraction efficiency of the planar structure and the defect structure with a variation in height.

In conclusion we demonstrated a quasi-planar single-photon source with a very high extraction efficiency of 42% ± 5%, in good agreement with theoretical values. The cavity is based on naturally occurring nanohills on planar microcavities, which are self aligned to the implemented QD emitters. Similar high photon outcoupling efficiencies in QD-microcavity systems have previously required complicated photonic resonator geometries, highly advanced lithography and perfect spatial alignment. The high extraction efficiency in our experiment can be attributed to an efficient guiding of the light into a collection objective provided by the defect structure. Due to the absence of any etched and exposed lateral semiconductor-air interfaces, such cavities have great potential for experiments and applications relying on extended spin-coherence times, or large scale coupling of neighboring QDs.

Acknowledgments

The authors gratefully thank M. Emmerling and T. Steinl for expert sample preparation. This work was financially supported by the German Ministry of Education and Research (BMBF) via the project QuaHL-Rep and by the State of Bavaria.

#205981 - $15.00 USD Received 4 Feb 2014; revised 13 Mar 2014; accepted 14 Mar 2014; published 31 Mar 2014